

Supercritical Disk Accretion with Mass Loss

Galina V. Lipunova
Sternberg astronomical Institute,
Universitetskii pr. 13, Moscow, 119899, Russia

galja@sai.msu.su

Abstract

We consider supercritical accretion onto a compact object when the accretion rate exceeds its value derived from the Eddington limit: $\dot{M}_{Edd} = L_{Edd}/c^2$. We use the scenario that was proposed by Shakura and Sunyaev (1973) for the supercritical regime, according to which matter flows out of the gas-disk surface under radiation pressure. An analytic solution of the accretion-disk structure is obtained for this scenario by using classical equations. An attempt is made to construct a model for nonconservative supercritical accretion with advection. To this end, we develop a numerical scheme for calculating the structure of an advective disk with mass outflow. The goal of solving the problem of a supercritical disk with mass loss is to explain accreting sources with outflowing envelopes, for example, SS 433 and galactic nuclei. The structure and observational manifestations of the envelope which forms around a supercritical disk are considered by taking into account bremsstrahlung absorption and Thomson scattering of photons.

Introduction

The accretion-disk theory is used in astrophysics to explain a wide range of X-ray sources, their energetics, spectra, and variability. By now a wide variety of models have been proposed to account for the observed characteristics of quasars, X-ray pulsars, and cataclysmic variables.

The disk-accretion studies by Gorbatskii (1964), Lynden-Bell (1969), Shakura (1972), Pringle and Rees (1972), and Shakura and Sunyaev (1973) yielded the first mathematical theory of accretion disks. The general pattern of steady-state accretion in disks is as follows: the gravitational energy of the gas that rotates around the central star transforms into the thermal and kinetic energy of orbital motion through friction. For the effective emission of heat, the gas flows cool down and produce a disk structure. The disk luminosity is a function of the central object's mass, the rate of accretion onto it (i.e., the rate of mass inflow to the outer boundary of the accretion disk from the interstellar medium or from a neighboring star), and the specific mechanism of angular-momentum transfer in the disk.

When the accretion rate is not too high, the total accretion-disk luminosity is directly proportional to the accretion rate. Under such quiet conditions, the global disk structure can be successfully described by the classical solution of Shakura and Sunyaev (1973).

However, it is well known from the scenario for the evolution of binaries (Tutukov and Yungelson 1973; Van den Heuvel 1994) that there are evolutionary stages of violent mass transfer between the component stars in binary systems. At \dot{M} greater than the critical value

$$\dot{M}_{cr} = L_{Edd}/\vartheta c^2 \simeq 2 \times 10^{-9} \frac{m}{\vartheta} M_{\odot}/\text{yr} , \quad (1)$$

where $m = M/M_{\odot}$ is the stellar mass (in solar masses), and ϑ is the accretion efficiency in a thin disk, the disk luminosity becomes so large that the radiation pressure begins to hamper the infall of matter to the center. This accretion regime is called supercritical or super-Eddington. In a spherically symmetric case, the luminosity reaches the Eddington limit, when the gravitational attraction by the central star equals the radiation pressure on a proton:

$$\frac{L_{Edd}}{4\pi r^2} \frac{\sigma_T}{c} = \frac{m_p M G}{r^2} , \quad L_{Edd} \approx 1.25 \times 10^{38} m \text{ erg/s} , \quad (2)$$

where $\sigma_T = 6.65 \times 10^{-25} \text{cm}^2$ is the cross section for Thomson scattering by free electrons.

In reality, the accretion rate clearly exceeds the critical value (1) in several cases. For example, in SS 433, matter from the supergiant flows onto the compact object (a neutron star or a black hole) at a rate of $\sim 10^{-4} M_\odot \text{yr}^{-1}$ (Cherepashchuk 1981). High accretion rates may occur in galactic nuclei during intense infall of stellar matter onto supermassive black holes (see, e.g., Dopita 1997; Szuszkiewicz et al. 1996).

Shakura and Sunyaev (1973) proposed a self-regulation mechanism for supercritical accretion. As soon as the luminosity of the disk exceeds the Eddington limit, matter flows out of its surface, causing the rate of accretion onto the central object to decrease. The amount of gravitational energy which can be liberated in the disk thus decreases, and the disk luminosity is limited by a value that does not greatly exceed the Eddington limit.

The outflow from the disk surface takes place inside the radius at which the disk thickness is equal in order of magnitude to the disk radius. The disk structure outside can be described by the classical Shakura–Sunyaev solution. This radius R_s is called the spherization radius. As was established by Shakura and Sunyaev (1973), if the accretion rate in the disk decreases as

$$\dot{M}(r) = \frac{r}{R_s} \dot{M}_o, \quad (3)$$

then the total disk luminosity does not greatly exceed the Eddington limit: $L_{tot} \sim L_{Edd} \times (1 + \ln(\dot{M}_o/\dot{M}_{cr}))$. In this case, the total mass loss rate in the wind is $\sim \dot{M}_o(1 - \dot{M}_{cr}/\dot{M}_o)$, where \dot{M}_o is the initial accretion rate at the outer disk radius.

The hypothesis of mass outflow from the disk is confirmed, for example, by photometric and spectroscopic observations of SS 433, which suggest the presence of an envelope of matter flowing out of the disk (e.g., Murdin et al. 1980). In some galactic nuclei, observations reveal outflow rates reaching $\sim 1 M_\odot/\text{yr}$ (Heckman et al. (1981).

The authors who consider the winds from accretion disks, for example, in cataclysmic variables, propose the mechanism of wind generation in spectral lines. The rate of mass loss by such disks is $\sim 10^{-11-12} M_\odot/\text{yr}$ at a flow rate of $\sim 10^{-8} M_\odot/\text{yr}$ (see, e.g., Suleimanov 1995; Pereyra et al. 1997). By contrast, for supercritical mass outflow, a large optical depth in the disk and the wind gives rise to a blackbody spectrum and causes this mechanism to

decrease in importance. Meier (1979) considered the wind generated by a supercritical disk at a certain radius close to the spherization radius (for the Shakura–Sunyaev disk model) and computed the vertical structure of the disk and the wind. Here, we consider the radial structure of an outflowing disk with height-averaged physical parameters. For SS 433, our outflow rate is comparable in order of magnitude to the value of Meier (1982): $3 \div 9 \times 10^{-6} M_{\odot}/\text{yr}$.

Equations for disk accretion with mass loss

The structure of accretion disks at subcritical accretion rates is described by standard equations of disk accretion (Shakura and Sunyaev 1973). In this case, the disk geometry can be roughly described by a thin disk, and appropriate simplifying assumptions, for example, replacement of the physical parameters in the disk by their height-averaged values, can be imposed on the equations. To describe a nonconservative disk — a disk with mass outflow from its surface, we use the equations from the standard model, which we modified to fit our view of mass outflow from the disk.

The equation of radial angular-momentum transfer along the disk — the φ component of the Euler equation integrated over the coordinate perpendicular to the disk plane, is

$$\frac{d}{dr}\{\dot{M}(r)\omega r^2\} = -2\pi \frac{d}{dr}\{W_{r\varphi}r^2\} + \frac{d\dot{M}(r)}{dr}\omega r^2, \quad (4)$$

Here, $\dot{M}(r)$ is the accretion rate, r is the radius, ω is the Keplerian angular velocity, and $W_{r\varphi}$ is the integrated, height-averaged tangential component of the stress tensor $w_{r\varphi}$ in the accretion disk:

$$W_{r\varphi} = 2Hw_{r\varphi} \quad w_{r\varphi} = -\eta r \frac{\partial \omega}{\partial r}, \quad (5)$$

where H is the disk half-thickness, and η is the dynamical viscosity. The change in angular momentum of the accreted gas is the sum of the angular-momentum transfer by viscosity (the first term on the right-hand side of (4)) and the transfer of angular momentum carried away by the outflowing matter (second term). This equation differs from the standard equation of

angular-momentum transfer (see Eq. (14)), in which $\dot{M} = \text{const}$, precisely by the presence of the second term on the right-hand side.

The turbulent viscosity can be described by the dynamical coefficient, $\eta \approx \rho \langle v_t l_t \rangle$, where v_t and l_t are the characteristic velocity and length of turbulent mixing, respectively. Using Prandtl's semiempirical relation

$$v_t = l_t r \frac{d\omega}{dr} ,$$

we find from (5) that

$$w_{r\varphi} \simeq -\rho v_t^2 = -m_t^2 \rho a^2 ,$$

where m_t is the Mach number, $m_t^2 = v_t^2/a^2$, and a is the speed of sound. Shakura (1972) introduced a turbulence parameter α , which relates the tangential component of the stress tensor to the pressure in the disk $P = P_{gas} + P_{rad}$ (the sum of the gas and radiation pressures):

$$w_{r\varphi} = -\alpha P . \quad (6)$$

The disk models that assume turbulence to be the source of viscosity and that use relation (6) are called α -disks.

The equation of energy balance: the mechanical energy due to viscosity produced in the disk at radius r is completely emitted at the same radius,

$$Q^+(r) = Q_{rad}(r) , \quad (7)$$

where $Q_{rad}(r)$ is the radiative flux from one of the two accretion-disk surfaces, and $Q^+(r)$ ($Q^+(r)$ (erg/cm²s) is half the heat released in a disk annulus of width dr .

$$Q^+(r) = -\frac{3}{4}\omega W_{r\varphi} , \quad Q_{rad} = \frac{1}{3} \frac{c}{k_T \rho H} \varepsilon_{rad} , \quad (8)$$

where $k_T = \sigma_T/m_p = 0.4 \text{ cm}^2/\text{g}$ is the specific Thomson scattering cross section ($m_p = 1.67 \times 10^{-24} \text{ g}$ is the proton mass), ε_{rad} is the mean radiative energy density, and ρ is the mass density. Equation (7) requires special stipulations in the case of a high accretion rate: it turns out that the heat exchange between a given portion of the disk and its adjacent portions must also be taken into account, as discussed below. Note that the "local" equation of energy balance (7) allows an analytic treatment of the problem with outflow.

The expression for Q_{rad} in (8) is the solution of the transfer equation in the diffusion approximation, which is valid for optically thick disks. The optical depth τ of such a disk, whose geometrical thickness can be determined from the condition that the vertical component of the gravity is equal to the pressure (hydrostatic equilibrium),

$$\frac{1}{\rho} \frac{dP}{dh} \sim \frac{P}{\rho H} = \frac{GMH}{r^3}, \quad (9)$$

is much larger than unity at supercritical accretion rates. Here, we disregard the general-relativity effects. Novikov and Thorne (1973) considered thin accretion disks around Schwarzschild black holes in terms of the general-relativity theory.

The equation of state

$$P = \rho a^2 = \frac{\varepsilon_{rad}}{3} \quad (10)$$

holds in the radiation-dominated regions of thin disks. In the supercritical regime, the radiation pressure in the disk is much higher than the gas pressure.

The spherization radius R_s at which mass outflow sets in can be approximately determined from the condition that the luminosity reaches the Eddington limit (Lipunov 1992):

$$\frac{1}{2} \frac{GM\dot{M}_o}{R_s} \approx L_{Edd}, \quad \text{then we have} \quad R_s \approx R_o \frac{\dot{M}_o}{\dot{M}_{cr}}, \quad (11)$$

where R_o is the radius of the inner disk boundary.

The matter flowing out of the disk surface produces an expanding envelope. The problem of mass outflow from a supercritical accretion disk is similar, except for the geometry, to the problem of outflow of strong winds from WR stars and giants. The wind structure is described by the continuity, momentum, and energy equations. We do not set the goal of solving this complex problem and use an upper limit to determine the outflow rate. For the matter from the disk to be moved to infinity, the work $d\dot{M} \left(\frac{GM}{r} - \frac{V_{Kepl}^2}{2} \right)$ must be done in a second. Clearly, an upper limit on $d\dot{M}$ can be placed by assuming that this power is equal to $2 Q_{rad} 2\pi r dr$, the luminosity of the disk annulus from the two surfaces. We thus obtain the following estimate, which

is the so-called “energy-wind” relation:

$$\frac{1}{2} \frac{d\dot{M}}{2\pi r dr} \frac{(v_\infty^2 - v_{Kepl}^2)}{2} \equiv \frac{\omega^2 r}{8\pi} \frac{d\dot{M}(r)}{dr} = Q_{rad} . \quad (12)$$

For the mass outflow from the disk, the accretion flux decreases with radius and is the sought-for function which is given by

$$\dot{M}(r) = 4\pi r H \rho v_r , \quad (13)$$

where v_r is the radial velocity in the disk.

Conservative solution

The solution to the set of equations (4) (without the second term on the right-hand side)–(10) is a classical solution for a thin accretion disk without outflow, which is called the standard model. In this case, the accretion efficiency is $\theta = 1/12$. The equations can describe the disk structure in different regions, depending on the form of equation of state, i.e., on the relative contribution of the radiation pressure and the gas pressure. The solution to the equation of angular-momentum transfer,

$$\frac{d}{dr} \{ \dot{M} \omega r^2 \} = -2\pi \frac{d}{dr} \{ W_{r\varphi} r^2 \} , \quad (14)$$

for $\dot{M} = \text{const}$ and the Keplerian law of motion $\omega = \sqrt{GM/r^3}$ is the following (Shakura and Sunyaev 1973)

$$W_{r\varphi} = \frac{\omega \dot{M}}{2\pi} \left(1 - \sqrt{\frac{R_{in}}{r}} \right) + W_{r\varphi}^{in} \left(\frac{R_{in}}{r} \right)^2 , \quad (15)$$

where R_{in} is the inner radius, and $W_{r\varphi}(R_{in}) \equiv W_{r\varphi}^{in}$. In the standard solution at the inner disk boundary $R_{in} = R_o$, one assumes that $W_{r\varphi}^{in} = 0$.

The total disk luminosity in this solution is proportional to the accretion rate,

$$L_{tot} = \frac{1}{2} \frac{\dot{M} GM}{R_o} = L_{Edd} \frac{\dot{M}}{\dot{M}_{cr}} , \quad \dot{M} < \dot{M}_{cr} . \quad (16)$$

If the central star is a Schwarzschild black hole, then $R_o = 3R_g$, the radius of the marginally stable orbit; if it is a neutron star, then the inner disk boundary lies either on the neutron-star surface¹ or at the Alfvén radius in the case of a strong magnetic field near the neutron star.

The disk thickness in the regions under consideration changes with radius only slightly, as we show below. The condition for radiation domination can be written as the equality of the forces of attraction and radiation pressure on the disk surface,

$$\frac{m_p G M H}{r^3} \approx \frac{Q_{rad} \sigma_T}{c} . \quad (17)$$

Using (7), (8), and (15), we obtain $Q_{rad}(r)$ and, after simple algebraic transformations, derive

$$H = R_g \frac{\dot{M}}{\dot{M}_{cr}} \frac{3}{4\vartheta} \left(1 - \sqrt{\frac{R_o}{r}} \right) \approx R_g \frac{\dot{M}}{\dot{M}_{cr}} \frac{3}{4\vartheta} \quad (r \gg R_o) . \quad (18)$$

Solution in a nonconservative model

The set of equations (4)–(13) describes the disk structure within the spherization radius, where mass outflow proceeds. Its solution can be found analytically. From Eqs. (4), (7), (8), and (12), we derive $\dot{M}(r)$ and $W_{r\varphi}$: the accretion rate in the disk, starting from the spherization radius R_s at which outflow sets in, falls off to the center as

$$\dot{M}(r) = \dot{M}_o(r) \left(\frac{R_s}{r} \right)^{3/2} \frac{1 + \frac{3}{2} \left(\frac{r}{R_o} \right)^{5/2}}{1 + \frac{3}{2} \left(\frac{R_s}{R_o} \right)^{5/2}} , \quad r \leq R_s . \quad (19)$$

This law has the asymptotic limit

$$\dot{M}(r) \approx \dot{M}_o(r) \frac{r}{R_s} \quad R_o \ll r \leq R_s ,$$

i.e., the derived solution matches Shakura–Sunyaev’s solution (Eq. (3)). The analytic expression for the height-averaged component of the stress tensor in

¹For a neutron star with a soft equation of state, the stellar radius may turn out to be smaller than the radius of the marginally stable orbit.

the disk is

$$W_{r\varphi} = - \frac{\dot{M}(r)\omega}{4\pi} \frac{1 - \left(\frac{r}{R_o}\right)^{5/2}}{1 + \frac{3}{2}\left(\frac{r}{R_o}\right)^{5/2}} . \quad (20)$$

The boundary conditions at the inner radius R_o are $W_{r\varphi} = 0$ and $Q_{rad} = 0$. The absence of stress at the inner disk edge is undoubtedly a simplifying assumption, which ignores the hydrodynamic pattern of the flow.

The full solution is obtained by joining the solution with outflow and the solution without outflow (outside the spherization radius), which is the standard Shakura–Sunyaev solution for the appropriate boundary conditions at the spherization radius R_s (Eq. (15)).

The spherization radius is a parameter of the problem. It can be numerically adjusted in such a way that the disk luminosity outside this radius is of the order of L_{Edd} :

$$R_s : \quad L(r > R_s, R_s) = L_{Edd} . \quad (21)$$

Note that the refined spherization radius gives a different total rate of mass outflow from the disk. Bisnovatyi-Kogan and Blinnikov (1977) studied the dynamics of particle motion near a transcritical disk and found that the process of particle escape to infinity under radiation pressure in the gravitational field of a central object or disk spherization is established at a total disk luminosity in the range 0.6 to $1L_{Edd}$. It was found that up to 80% of the matter could be carried away from the disk for $0.6L_{Edd}$. However, since R_s is currently rather uncertain, we use condition (21) in the numerical procedure.

In Fig. 1, the solid lines represent some of the disk characteristics as a function of radius for $\dot{m} \equiv \dot{M}/\dot{M}_{cr} = 1000$; the change in accretion rate, which is described by Eq. (19), is shown in the lower left panel; the derived spherization radius is $R_s = 1.62 R_o \dot{M}_o/\dot{M}_{cr}$ (cf. Eq. (11)).

The upper left panel shows a plot of the relative half-thickness H/r in the disk against radius, which is constant (solid line) for $r < R_s$ and is the same for any $\dot{M}_o > \dot{M}_{cr}$. This can be easily verified by substituting the accretion rate $\dot{M}(r)$, which decreases under the effect of the energy-wind mechanism (19), into the expression for the disk thickness in the radiation-dominated region (18).

Advective disks with mass loss

Formulation of the Problem and Results

At supercritical accretion rates, the disks are always thick. The assumption that $H/r \ll 1$ is invalid for them. This can be illustrated by an analytical solution for a nonconservative disk: we see from Fig. 1 (upper left panel, solid line) that the relative half-thickness reaches ~ 0.6 .

In a thick disk, the emission from the surface is not an efficient cooling mechanism. In the characteristic time of inward matter motion along the radius, the heat cannot radiate away and is transported with the matter, i.e., the time it takes for a photon to reach the disk photosphere, $t_{\text{dif}} = 3H\tau/c$ (here, $\tau = H\bar{n}\sigma_T \gg 1$ is the optical depth for scattering across the disk, and \bar{n} is the height-averaged number density of the disk matter), is much longer than the characteristic time of radial particle motion r/v_r , where $v_r \sim \alpha \left(\frac{H}{r}\right)^2 \omega r$ is the radial velocity with which the matter moves over the disk (see Fig. 2).

This transport of heat along the disk with matter is called advection. If advection is taken into account, the equation of energy balance (7) changes:

$$Q^+ = Q_{\text{rad}} + Q_{\text{adv}} , \quad Q_{\text{adv}} = \rho v_r H T \frac{dS}{dr} , \quad (22)$$

where T is the temperature, and S is the specific entropy. Using standard thermodynamic relations, the expression for advection can be rewritten as

$$Q_{\text{adv}} = \rho v_r H \frac{d\left(\frac{\varepsilon}{\rho}\right) + P d\left(\frac{1}{\rho}\right)}{dr} , \quad (23)$$

where ε is the internal energy density of the gas, and P is the total gas pressure (averaged over H). Inside the disk, where the optical depth is much larger than unity, the photons and particles are in thermodynamic equilibrium, and $\varepsilon = AT^4$, $A = 7.58 \times 10^{-15} \text{erg/cm}^3$. Since the radiation pressure dominates over the gas pressure in supercritical disks, we have

$$P \approx P_{\text{rad}} = \frac{AT^4}{3} . \quad (24)$$

Thus, the set of equations (4)–(6), (8), (9), (12), (13), and (22)–(24) describes an outflowing disk with advection. A numerical solution of the

disk structure can be found by using a developed computer code, which has two modifications: to compute the structure of an advective disk with and without outflow. We tested the numerical scheme on the Shakura–Sunyaev standard-disk model.

The results of our calculations for the accretion rate $\dot{M}_o/(12L_{Edd}/c^2) = 1000$ are shown in Fig. 1 (long dashes). The short dashes represent the results of our calculations for a conservative advective disk: no mass loss by the disk, and the accretion rate is constant.

As we see, in the solutions with advection, it dominates in the inner disk regions, i.e., only a small fraction of the heat is emitted: $Q_{rad}/Q^+ \ll 1$. In this region, the disk cooling by the energy wind (Eq. (12)) is inefficient. Nevertheless, it is clear that a considerable fraction of the initial accretion rate can be lost by the disk (long dashes).

Our numerical calculations for various \dot{m} in the range 10^2 – 10^4 yielded

$$L_{tot}/L_{Edd} \approx 0.6 + 0.7 \ln \dot{m} . \quad (25)$$

Figure 3 shows plots of the accretion rates in the disk for various values at the outer disk boundary.

Observations of SS 433 reveal an expanding envelope around the accretion disk. The binary system SS 433 consists of an O or B star and a compact object (a black hole, $M \sim 10M_\odot$, or a neutron star, $M \sim 1M_\odot$) (see, e.g., Van den Heuvel 1981). Mass accretion onto the compact object on the thermal time scale of a normal star proceeds in the system at a rate of 10^{-4} – $10^{-3}M_\odot/\text{yr}$ (Cherepashchuk 1981; Van den Heuvel 1981). The mass loss rate in the envelope is 10^{-5} – $10^{-4}M_\odot/\text{yr}$ (Shklovskii 1981; Dopita and Cherepashchuk 1981; Van den Heuvel 1981).

Thus, the observed outflow rate from the system, which is comparable to the accretion rate, is obtained in the model of a supercritical nonconservative disk.

Envelope around a supercritical disk

Luminosity and Effective Temperature

The envelope that is formed from the matter flowing out of a supercritical disk can be optically thick for the emission from the inner disk regions. Its X-ray emission is reprocessed into a softer emission. Let us roughly estimate the

effective temperature and emergent luminosity of the envelope as a function of the model parameters and the empirically derived quantities

$$A_1 = \frac{\dot{M}_{en}}{\dot{M}_o} , \quad A_2 = \frac{R_s}{\dot{m}R_o} , \quad A_3 = \frac{R_o}{R_g} . \quad (26)$$

The first two coefficients are determined when the disk structure is calculated numerically; \dot{M}_{en} is the mass loss rate in the envelope; \dot{M}_o is the initial accretion rate at the outer disk boundary; R_o is the inner disk radius; R_s is the spherization radius which is derived from condition (21); and the third coefficient is equal to 3, if the compact accreting object is a black hole, and is set approximately equal to 3 in the case of a neutron star:

$$A_1 \simeq 0.5 , \quad A_2 = 0.87 , \quad A_3 = 3 .$$

We assume that the mass outflow proceeds at a constant rate

$$\dot{M}_{en} = 4\pi R_s^2 m_p n_s v_\infty(R_s) , \quad (27)$$

where n_s is the number density in the envelope at radius R_s , and $v_\infty(R_s) = \sqrt{2GM/R_s} = 0.62 c \dot{m}^{-1/2}$ is the outflow rate.

The emergent spectrum differs in shape from a blackbody spectrum, because the scattering of emergent photons by free electrons plays a major role in the opacity (Shakura and Sunyaev 1973; Sunyaev and Shakura 1974). The visible envelope radius is R_T , where the photon is scattered for the last time. The radius R_T can be derived from the relation

$$\tau_T(R_T) \equiv \int_{R_T}^{\infty} \sigma_T n_s dr = \frac{\sigma_T n_s R_s^2}{R_T} = 1 , \quad (28)$$

by taking into account the fact that the particle number density in the envelope at a constant outflow rate in it falls off as the inverse square of the distance. From (26)–(28) we obtain

$$R_T = 1.77 \times 10^6 A_1 \sqrt{A_2 A_3 \dot{m} \dot{m}^3} \text{ cm} . \quad (29)$$

At frequencies at which scattering is larger than absorption, the emergent spectrum from the last scattering surface is (Zeldovich and Shakura 1969)

$$F_\nu = \left(\frac{k_{ff}}{4\sigma_T^2 R_T} \right)^{1/4} \pi B_\nu(T) , \quad (30)$$

where $k_{ff} = 3.69 \times 10^8 T^{-1/2} \nu^{-3} g(1 - e^{-h\nu/kT}) \text{ cm}^5$ is the bremsstrahlung absorption coefficient, $B_\nu(T)$ is the Planck function, g is the Gaunt factor, T is the envelope temperature, and ν is the frequency of the emergent emission. The shape of the spectrum determines the observed color temperature of the envelope. The temperature derived from Wien's displacement law (which is occasionally used instead of the color temperature) is mainly determined by the plasma temperature ; m and \dot{m} actually affect only the flux and shape while leaving the position of the peak in the spectrum unchanged (at those values at which the emergent spectrum is not a blackbody spectrum near the peak) (see (30) and Fig. 4). The frequency-integrated expression (30) yields the flux $Q = 54 R_T^{-1/4} T^{25/8} \text{ erg/s cm}^2$ (the Gaunt factor is set equal to 1) and is an analog of Stefan-Boltzmann's law (Sunyaev and Shakura 1974). The envelope luminosity is then

$$L = 4\pi R_T^2 Q = 2.15 \times 10^{36} T_4^{25/8} R_{12}^{7/4} \text{ erg/s} , \quad (31)$$

where $T_4 = T/10^4 \text{ K}$ and $R_{12} = R_T/10^{12} \text{ cm}$. The departures from Stefan-Boltzmann's law become significant at $T > 2.3 \times 10^3 R_{12}^{-2/7} \text{ K}$. Assuming that the spectrum has a nonblackbody shape (i.e., when scattering dominates), if $k_\nu < 4\sigma_T^2 R_T$, we find that this condition for the emission at $\lambda = 5500 \text{ \AA}$ takes the form $\dot{m} > 186 m^{-2/3}$ (see also Fig. 5). Using (29), we thus obtain

$$L = 1.8 \times 10^{26} (A_1 \sqrt{A_2 A_3})^{7/4} m^{7/4} \dot{m}^{21/8} T_4^{25/8} \text{ erg/s} . \quad (32)$$

SS 433

Object no. 433 from the catalog of Stephenson and Sanduleak (1977) is famous primarily for the two oppositely directed jets which move at a velocity of $0.26c$ (Fabian and Rees (1979). According to the current model, the jets are generated at the center of an accretion disk around one of the components of the close binary system, in which supercritical accretion takes place. Mass flow onto the compact object proceeds in the binary on the thermal time scale of a normal star at a rate of 10^{-4} – $10^{-3} M_\odot/\text{yr}$ (Cherepashchuk 1981; Van den Heuvel 1981). The mass loss rate in the envelope is 10^{-5} – $10^{-4} M_\odot/\text{yr}$ (Shklovskii 1981; Dopita and Cherepashchuk 1981; Van den Heuvel 1981). Assuming a lower limit on the flow rate, we find from (1) that the following

relation holds for SS 433:

$$m\dot{m} \approx 4.7 \times 10^4 \vartheta , \quad (33)$$

where $\dot{m} = \dot{M}_o/M_{cr}$, and ϑ is the accretion efficiency in a thin disk (bears no direct relation to the actual accretion efficiency, which is $L_{tot}/(\dot{M}_o c^2) = 1/\dot{m}(\vartheta L_{tot}/L_{Edd})$).

For our estimates we consider two cases: (1) $m = 10$, $\dot{m} = 1000$; and (2) $m = 1 \div 2$, $\dot{m} = 10000$. However, a black hole and a neutron star as the compact object represent markedly different situations, because, in contrast to a neutron star, a black hole has an event horizon under which the matter and energy accreted in an advective disk can freely fall. From (25) we derive the total luminosities of outflowing advective accretion disks: (1) $L_{tot} \approx 5.4 L_{Edd,BH} \approx 7 \times 10^{39}$ erg/s (black hole) and (2) $L_{tot} \approx 7.0 L_{Edd,NS} \approx 9 \times 10^{38}$ erg/s (neutron star). For supercritical accretion onto a neutron star, the bulk of the energy from the magnetospheric region can be carried away by neutrinos (Basko and Sunyaev 1976).

Using (33) and (29), we can find a relation between the uncertain mass of the compact object in SS 433 and the radius of the visible envelope (see Fig. 6):

$$R_{12} \approx 14.6 \vartheta^{3/2} m^{-1/2} . \quad (34)$$

Various theoretical and observational estimates yield an expanding-envelope radius of $\sim 10^{11}$ – 10^{12} cm for SS 433 (see, e.g., Fabrika 1984; Bochkarev and Karitskaya 1985).

In the envelope of SS 433 for $m = 10$ and $\dot{m} = 1000$ or even for $m = 1 \div 2$ and $\dot{m} = 10000$, electron scattering dominates over absorption (Fig. 5). The color temperature determined from the peak flux from SS 433 (Murdin et al. 1980) is ~ 25000 K, which corresponds to the plasma temperature in the envelope $T = 3.5 \times 10^4$ K (Fig. 4). From (32) we then derive $L \approx 3 \times 10^{37}$ erg/s for $m = 10$ and $L \approx 1 \times 10^{38}$ erg/s for $m = 2$. This luminosity estimate depends on the mass flow rate in the envelope. The formula $v_\infty(R_s) = 0.62 c \dot{m}^{-1/2}$ yields ~ 6000 km/s for $10M_\odot$. The observed Doppler widths of the “stationary” H α and He II lines are $\sim (1 - 2) \times 10^3$ km/s.

Conclusion

Here, we considered supercritical accretion onto a compact object. As a result, we obtained an analytic solution of the accretion-disk structure using classical equations. We developed a numerical scheme for calculating the accretion-disk structure with advection, i.e., with radial heat transport by the accreted matter. We obtained an estimate of the visible radius and luminosity of the envelope composed of outflowing matter as a function of the rate of accretion onto a black hole by taking into account bremsstrahlung absorption and Thomson scattering of photons.

The physical quantities in the equations we considered were averaged over the height. Finding an exact solution is a difficult and interesting problem, which requires considering two-dimensional hydrodynamic equations and which may also be associated with the problems of the generation of jets from sources with black holes.

Here, we also assumed that the orbital particle velocity was described by Kepler's law. In this case, we ignored the contribution of pressure to the equation of motion (we took into account the pressure only when we calculated the vertical disk structure, Eq. (9)). In distant regions, at $r \gg R_o$, this is quite acceptable. In Fig. 7, the speed of sound, the radial velocity over the disk, and the orbital Keplerian velocity $\sqrt{GM/r}$ are plotted against radius. Near the sonic point, i.e., at the distance at which the speed of sound is equal to the radial velocity, $a = v_r$, the contribution of pressure is large, and, as we see, the orbital and radial velocities are of the same order of magnitude there, i.e., the particle orbits cease to be Keplerian.

The energy-wind equation differs from the relation that is used in the standard stellar-wind theory,

$$m_p v \sim \frac{L}{c} . \quad (35)$$

If this law is used, then the efficiency of mass outflow from the disk decreases by several order of magnitude. Figure 8 shows the results of our numerical calculations for an advective disk with mass outflow that follows the law (35). It turns out that using this law generally reduces the outflow efficiency by more than two orders of magnitude and apparently cannot explain the rates of mass outflow from SS 433, which are comparable to the accretion rate in this system.

A distinctive feature of advective disks is that only a small fraction of the liberated gravitational energy of the accreted matter is emitted, while the heat is mainly transported in the disk. If the central star is a black hole, then matter together with energy fall into it without returning. By now the accretion-disk theory has progressed appreciably and has been applied to observed sources. It turns out that advection can be of considerable importance in supercritical accretion and at low accretion rates (see, e.g., Abramowicz et al. 1988, 1991; Narayan and Yi 1994; Narayan et al. 1997). In particular, in the opinion of these authors, the model of a subcritical, optically thin, two-temperature advection-dominated disk around a supermassive black hole can explain the observations of low-luminosity galactic nuclei (Narayan et al. 1995; Lasota et al. 1996).

Observations of SS 433 show that the disk loses up to 90% of the matter flowing to its outer boundary, producing an outflowing envelope around the compact star. Thus, the problem of calculating the structure of a nonconservative accretion disk arises. In this paper, we considered an approximate solution of this problem. We found numerical solutions to this simplified problem (one-dimensional, etc.) with advection for a wide range of accretion rates above the critical value. We thus show that, in principle, substantial loss of the accreted matter from the accretion disk is possible, and calculate its value.

ACKNOWLEDGMENTS

I wish to thank N.I. Shakura, V.M. Lipunov, and M.E. Prokhorov for a helpful discussion and the referees for useful critical remarks. I also wish to thank V. Astakhov and N. Lipunova for help in preparing the paper. This study was supported by the International Program for Education in the Field of Exact Sciences, the Russian Foundation for Basic Research (project no. 98-02-16801), and the Astronomy Science and Technology Program (1.4.2.3 and 1.4.4.1).

References

- [1] Abramowicz M.A., Bao G., Lanza A., Zhang X.-H. // *Astron. Astrophys.*, 1991, V. 245, P. 454.

- [2] Abramowicz M.A., Czerny B., Lasota J.P., Szuszkiewicz E. // *Astrophys. J.*, 1988, V.332, P. 646.
- [3] Basko M. M., Sunyaev R.A. // *MNRAS*, 1976, V. 175, P. 395.
- [4] Bisnovatyı–Kogan G.S., Blinnikov S.I. // *Astron. Astrophys.*, 1977, V. 59, P. 111.
- [5] Bochkarev N. G., Karitskaya E. A. // *Radio stars, Workshop on Stellar Continuum Radio Astronomy*, Boulder, 1984, Dordrecht: D. Reidel Publishing Co., 1985, P. 325.
- [6] Cherepashchuk A.M. // *MNRAS*, 1981, V. 194, P. 761.
- [7] Dopita M.A. // *Publ. Astron. Soc. Austr.*, 1997, V. 14, P. 230.
- [8] Dopita M.A., Cherepashchuk A.M. // *Vistas Astron.*, 1981, V.25, P. 51.
- [9] Fabian A.C., Rees M.J. // *MNRAS*, 1979, V. 187, P. 13.
- [10] *Fabrika S.N.* // *Soviet Astronomy Letters*, 1984, V. 10, P. 16.
- [11] Gorbatskii V.G. // *Sov. Astron.*, 1964, V. 8, P. 680.
- [12] Heckman T., Miley G.K., van Breugel W.J.M. // *Astrophys. J.*, 1981, V. 247, P. 403.
- [13] Lasota J.-P., Abramowicz M.A., Chen X., Krolik J., Narayan R., Yi I. // *Astrophys. J.*, 1996, V. 462, P. 442.
- [14] Lipunov, V.M. // 1992, *Astrophysics of Neutron Stars*, Springer Verlag,
- [15] Lynden–Bell D. // *Nature*, 1969, V. 233, P. 690.
- [16] Meier D.L. // *Astrophys. J.*, 1979, V. 233, P. 664.
- [17] Meier D.L. // *Astrophys. J.*, 1982, V. 256, P. 706.
- [18] Murdin P., Clark D.H., Martin P.G. // *MNRAS*, 1980, V. 193, P. 135.
- [19] Narayan R., Yi I. // *Astrophys. J.*, 1994, V. 428, P. L13.

- [20] Narayan R., Garcia M.R., McClintock J.E. // *Astrophys. J.*, 1997, V. 478, P. 79.
- [21] Narayan R., Yi I., Mahadevan R. // *Nature*, 1995, V. 374, P. 623.
- [22] Novikov I.D., Thorne K.S. // *Black Holes* (ed. DeWitt C., DeWitt B.), New York: Gordon & Breach, 1973, P. 343
- [23] Pereyra N.A., Kallman T.R., Blondin J.M. // *Bull. Am. Astron. Soc.*, 1997, V. 191, P. 12905.
- [24] Pringle J.P., Rees M.J. // *Astron. Astrophys.*, 1972, V. 21, P. 1.
- [25] Stephenson C.B., Sanduleak N. // *Astrophys. J.*, 1977, V. 33, P. 459.
- [26] Sunyaev R.A., Shakura N.I. // *Astron. Zhurnal*, 1974, V. 51, P. 102.
- [27] Tutukov A.V., Yungelson L.R. // *Nauchn. Inform. Astron. Sov.*, 1973, V. 27, P. 70.
- [28] van den Heuvel E.P.J. // *Vistas Astron.*, 1981, V. 25, P. 95.
- [29] van den Heuvel E.P.J. // *Interacting Binaries* (by Shore S.N., Livio M. and van den Heuvel E.P.J.), Springer-Verlag, 1994, P. 263.
- [30] Shakura N.I. // *Astron. Zhurnal.*, 1972, V. 49, P. 921.
- [31] Shakura N.I., Sunyaev R.A. // *Astron. Astrophys.*, 1973, V. 24, P. 337.
- [32] Shklovskii I.S. // *Sov. Astronomy*, 1981, V. 25, P. 315.
- [33] Suleimanov V.F. // *Astronomy Letters*, 1995, V. 21, P. 126.
- [34] Szuszkiewicz E., Malkan M.A., Abramowicz M.A. // *Astrophys. J.*, 1996, V. 458, P. 474.
- [35] Zeldovich Ya.B., Shakura N.I. // *Astron. Zhurnal*, 1969, V. 46, P. 225.

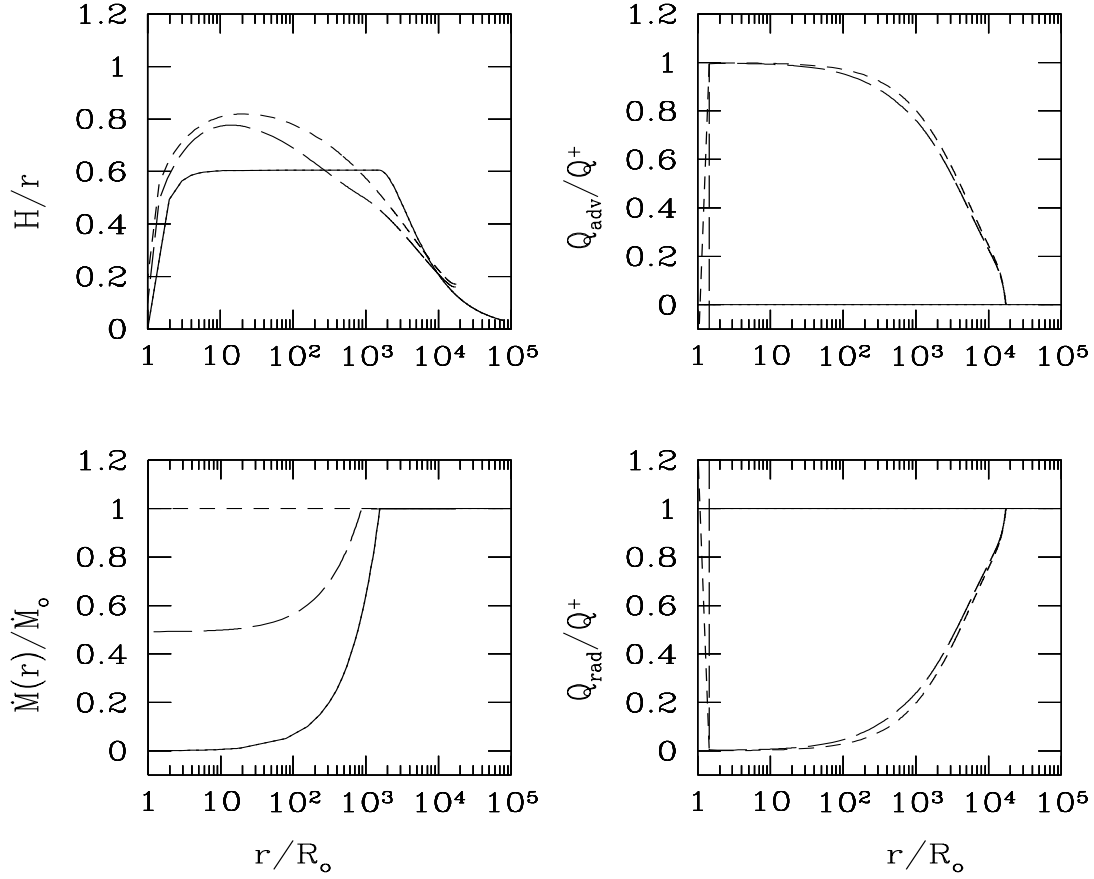


Figure 1: Relative thickness, accretion rate, fractions of emitted heat and advection versus radius. The solid line, the line with short dashes, and the line with long dashes represent an analytic solution with outflow, and advective conservative disk, and an advective nonconservative disk, respectively. The distance is normalized to the inner disk radius; $\dot{m} = 1000$.

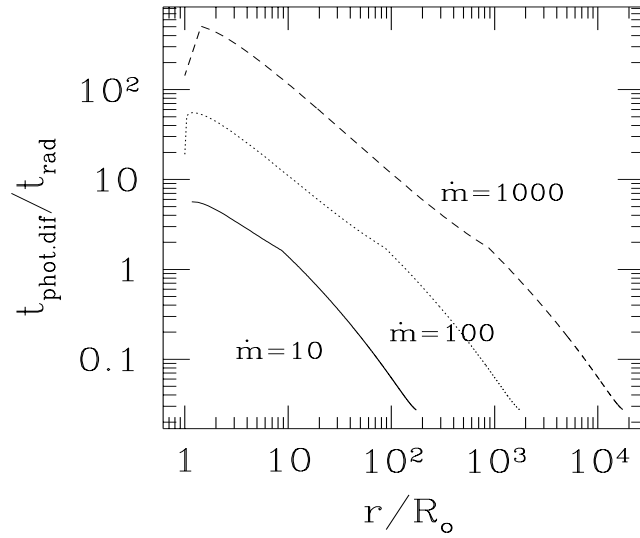


Figure 2: Ratio of the time of photon diffusion to the surface to the characteristic time of radial matter motion in the disk versus radius. The numerical calculations were performed for a nonconservative disk with advection; $\dot{m} = 10, 100, 1000$ and $\alpha = 0.5$.

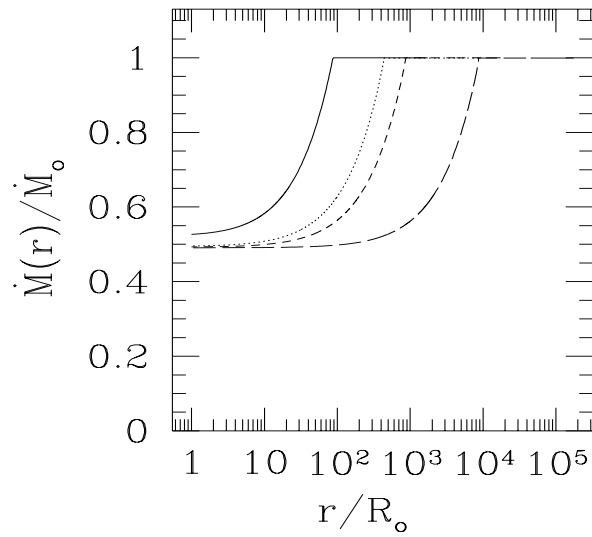


Figure 3: Change of the accretion rate in the disk due to mass outflow for various initial accretion rates. The curves (from left to right) represent the numerical calculations for an advective disk with $\dot{m} = 100, 500, 10^3, 10^4$.

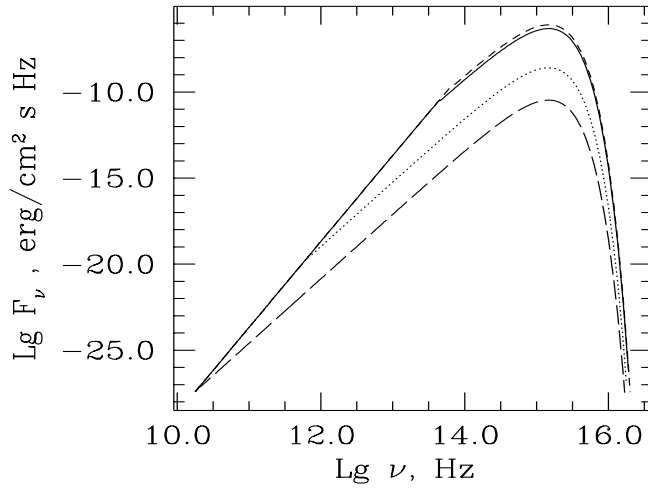


Figure 4: Spectrum of the envelope: a blackbody spectrum at low frequencies; the emergent flux decreases with increasing frequency, when electron scattering begins to dominate over bremsstrahlung absorption. The spectra are given for $m = 2$, $\dot{m} = 5000$ and $m = 10$, $\dot{m} = 1000$ (two upper close curves); $m = 10^8$, $\dot{m} = 10$ (middle curve); and $m = 10^8$, $\dot{m} = 10^3$ (lower curve). The plasma temperature in the envelope is $T = 3.5 \times 10^4$ K. The temperature derived from Wien's displacement law is $\approx 2.5 \times 10^4$ K.

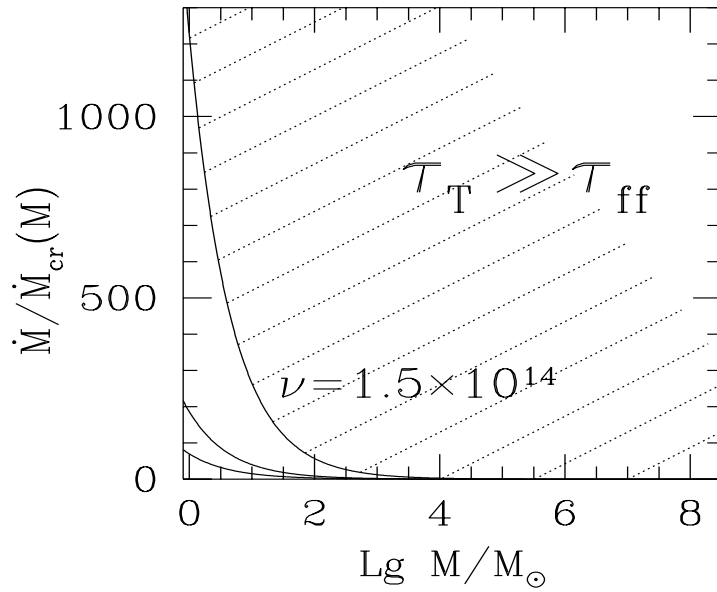


Figure 5: Curves that represent the lower boundaries of the domains of (m, \dot{m}) values in which the optical depth for scattering is larger than the optical depth for absorption at $\nu = 10^{15}$ Hz (lower curve), $\nu = 4.5 \times 10^{14}$ Hz (middle curve), and $\nu = 1.5 \times 10^{14}$ Hz (upper curve).

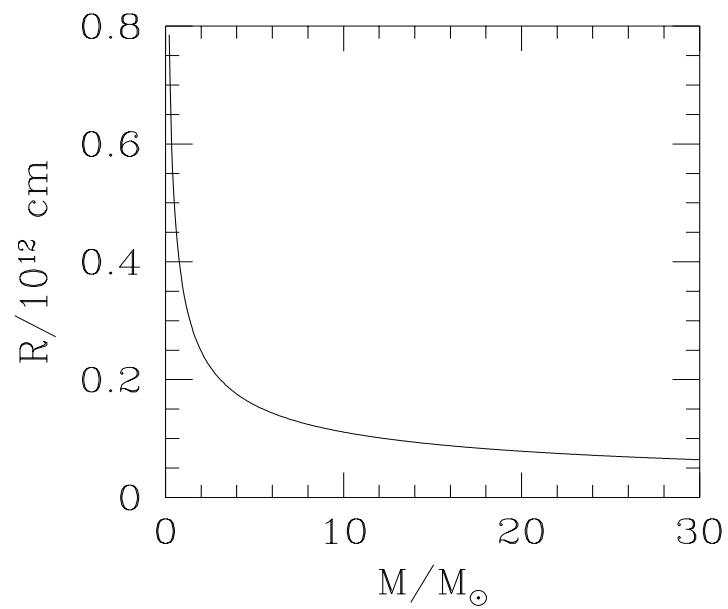


Figure 6: Visible envelope radius versus unknown mass of the compact component in SS 433.

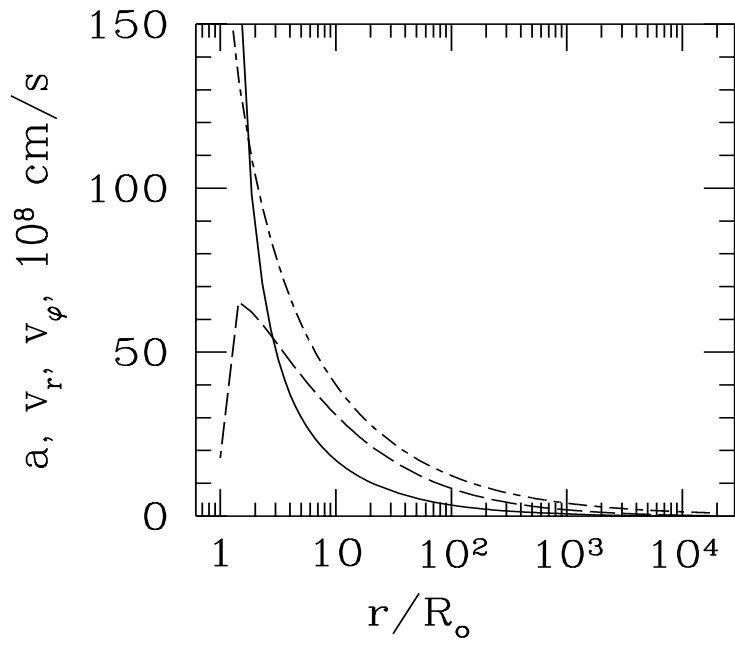


Figure 7: Speed of sound a (solid line), radial velocity in the disk v_r (long dashes), and Keplerian velocity v_ϕ (dot-dashed line) versus radius. The numerical calculations were performed for a nonconservative disk with advection for $m = 10$, $\dot{m} = 1000$, and $\alpha = 0.5$.

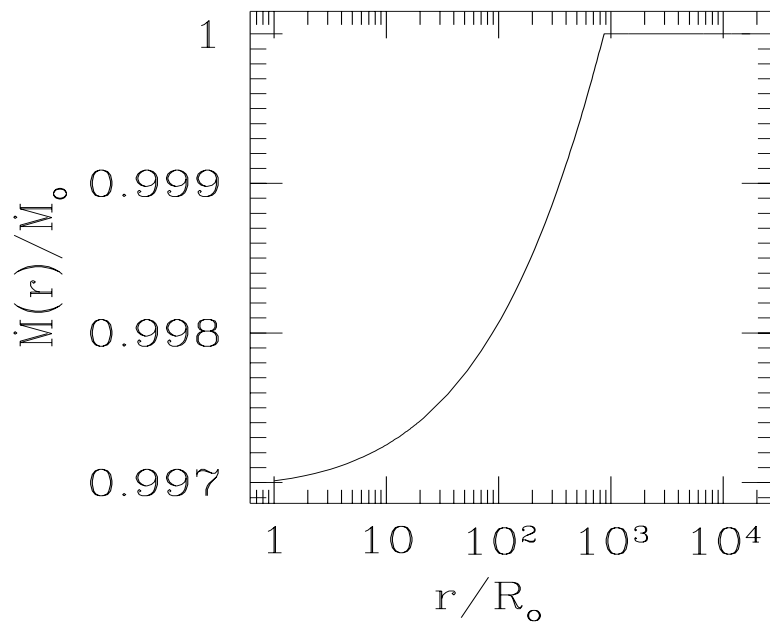


Figure 8: Ratio of the accretion rate in the disk to the initial accretion rate versus radius for mass outflow that follows the law (35). The numerical calculations were performed for an advective disk with $m = 10$ and $\dot{m} = 1000$.